Dual-Wavelength Vat Photopolymerization with Dissolvable, Recyclable Support Structures

Nicholas S. Diaco[1], Carl J. Thrasher[2], Max M. Hughes[1], Kevin A. Zhou[2], Michael N. Durso[2], Saechow Yap[1], Robert J. Macfarlane[2], A. John Hart[1]*

Affiliations:

[1]Department of Mechanical Engineering, Massachusetts Institute of Technology; Cambridge, MA 02139, USA.

[2]Department of Materials Science and Engineering, Massachusetts Institute of Technology; Cambridge, MA 02139, USA.

*Corresponding author. Email: ajhart@mit.edu

Abstract: Vat photopolymerization (VP) is widely used for additive manufacturing due to its speed, precision, and material versatility. However, traditional support structures limit printable geometries, require manual post-processing, and produce non-recyclable waste. We introduce a wavelength-selective resin for VP that enables single-vat, multi-material printing with dissolvable supports. Exposure to one wavelength produces a rigid, dissolvable thermoplastic, while a second wavelength forms a crosslinked thermoset resistant to dissolution. This selective solubility vat photopolymerization (SSVP) process allows for the fabrication of complex objects with support structures removable using non-toxic solvents like mineral oil. Heat treatment further tailors crosslink density and solubility. Dissolved supports can be recycled into fresh resin and reprinted without mechanical property loss, eliminating waste and paving the way for fully automated, sustainable manufacturing workflows.

Introduction

Additive manufacturing (AM) – the creation of physical objects layer-by-layer from digital data – enables the on-demand production of components with a variety of materials and with complex geometries (*1*). Vat photopolymerization (VP), an AM method that creates three-dimensional objects via light-induced polymerization of a liquid resin, has been widely adopted due to its material versatility, high resolution, and relatively high throughput. As a result, VP is widely used in dentistry, jewelry, footwear, and other consumer industries that require customized production at scale (*2–4*).

The layer-by-layer approach of VP can leave some features disconnected or weakly attached to the main structure until the print is complete. To address this, support structures are needed to stabilize these features during printing. The removal of supports after printing introduces additional manual labor steps, diminishes surface finish, and makes geometries with complicated cavities and channels challenging or impossible to print (*5*). Further, because VP typically uses feedstock resins that polymerize into non-processable thermosets, printing with support structures produces waste that cannot be recycled.

While new methods of volumetric VP can create small objects without support structures, volumetric approaches have not yet achieved the part size or level of detail possible with traditional VP printing (*6, 7*). Other methods of polymer AM using extrusion or inkjet deposition enable multiple materials to be deposited to permit selectively soluble supports (*8*), but the rheological, geometric, and material constraints of extrusion and jetting processes limit printing speed, dimensional resolution, and material diversity compared to VP (*9, 10*). Therefore, methods to simplify and improve the support removal process in VP would greatly empower the field of additive manufacturing.

In principle, selective dissolution of support structures is an ideal means to enable support removal in VP, as it could be performed by simply immersing the printed structure in a suitable solvent. With VP, dissolvable thermoplastics can be printed without crosslinkers using select, rapidly curing monomers (*11–13*). Because these materials are not crosslinked, they could be suitable as dissolvable support structures if printed alongside a non-dissolvable material for the final 3D printed part (*14*). However, because VP relies on resin vats, selectively incorporating both dissolvable supports and non-soluble materials in a single print requires mechanically complex vat- or resin-switching systems (*15, 16*).

Ideally, selective removal of predetermined portions of a VP-produced structure could be achieved with a single resin that could be printed into distinct solid compositions by using different wavelengths of light (*17–20*). For instance, two wavelengths of light can independently trigger cationic and free radical polymerizations in VP, leading to marked gradients in mechanical properties (*21–24*). If these final solids possessed orthogonal solubility in selected solvents, support structures could be intentionally programmed to dissolve after printing, leaving the other printed composition intact. To achieve wavelength-selective, multi-material printing of both dissolvable and insoluble components, the dissolvable polymer networks must be strong enough to support a printed part but also minimally crosslinked to permit rapid dissolution. Additionally, the process must ensure that the two materials have high interfacial strength during printing to stabilize all intermediate print states, but still be readily separated without disrupting the final solid network or introducing roughness to the printed structure's surface finish.

Materials and printing process

We introduce a single photoresin for VP that selectively forms either a thermoplastic or a thermoset depending on the illumination wavelength (Fig. 1). The main component of this resin is isobornyl acrylate (IBOA, ~60 wt%), which forms a rigid thermoplastic poly(IBOA) upon photopolymerization. Poly(IBOA) is readily dissolved in many organic solvents, but is minimally soluble in its precursor monomer under ambient conditions, ensuring that dissolution does not occur during printing (*11*). The second primary component of the resin is 3,4-epoxycyclohexylmethyl- 3,4-epoxycyclohexane carboxylate (EPOX, ~40 wt%), a difunctional epoxide that can form a solvent-resistant thermoset via cationic ring-opening polymerization. Concurrent printing of both dissolvable poly(IBOA) support features and non-dissolvable dual-network solids is achieved by incorporating two polymerization initiators that respond to different wavelengths of light. A free radical photoinitiator with absorption in the UV and low-wavelength portion of the visible spectrum allows printing of just poly(IBOA) under visible light (405 nm) irradiation. By also including a photoacid generator that responds only to UV light (365 nm), UV irradiation simultaneously polymerizes both IBOA and EPOX monomers. Additionally, including a small amount (~1 wt%) of the difunctional acrylate- and epoxide-containing crosslinker 3,4-epoxycyclohexylmethyl acrylate (ECHA), crosslinks between the two polymer networks are formed during UV exposure, increasing solvent resistance of the final printed construct.

Using this formulated resin, selective solubility vat photopolymerization (SSVP) was performed using a multi-wavelength projector-based printer with independent control of UV (365 nm) and visible (405 nm) light (Fig. S1). After printing, components produced under 405 nm illumination were soluble in many common solvents, including mineral oil (baby oil), D-limonene, mineral spirits, turpentine (paint thinner), and toluene; parts produced under 365 nm illumination were resistant to dissolution in these same solvents. Additionally, both the visible- and UV-cured materials demonstrated good mechanical properties directly after printing, with elastic moduli of 1.1 GPa and 1.8 GPa, respectively.

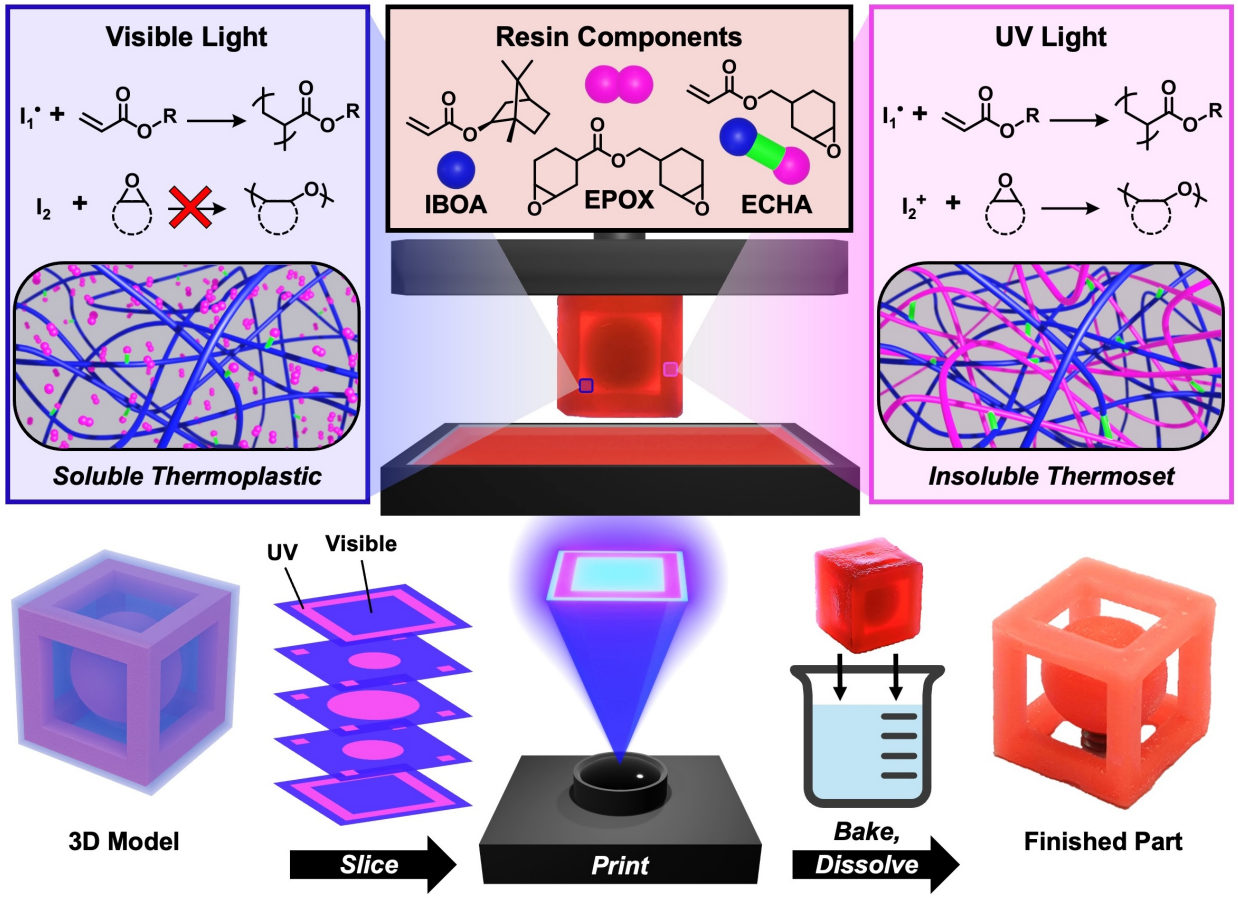

Fig. 1. Chemistry and process flow for selective solubility vat photopolymerization (SSVP) 3D printing. In the resin, visible light (405 nm) initiates free radical polymerization, forming a solid, dissolvable thermoplastic polymer. Exposure to UV light (365 nm) initiates free radical and cationic polymerization, resulting in a crosslinked, dissolution-resistant network after heat treatment. After printing, the thermoplastic can be dissolved away, leaving the finished thermoset part.

Thermal effects on network behavior

While this strategy enabled local control over solubility, the UV-exposed regions were still slightly soluble directly after printing, negatively affecting print resolution and surface finish. We attributed this partial solubility to vitrification preventing the full conversion of epoxides (*25*), and post-printing thermal treatments were therefore explored for further curing of epoxides (Fig. 2). Dynamic mechanical analysis (DMA) revealed that UV-exposed samples continued curing from 80°C to 150°C, with minimal additional curing at higher temperatures (Fig. S2). Dissolution studies revealed that solvent resistance in UV-exposed regions scaled with the maximum temperature reached during heat treatment (see supplementary text, fig. S3, and fig. S4 for details on dissolution studies). Increasing the treatment temperature above 150-160°C, however, resulted in incomplete removal of visible-exposed regions upon solvent exposure. A ramped heat treatment up to a temperature of 150°C was thus selected (Fig. 2, C and D). The elastic moduli of the visible- and UV-cured parts increased to 2.5 GPa and 2.6 GPa, respectively, after thermal treatment (Fig. S5 and fig. S6).

To better understand the mechanisms underlying thermal post-processing, monomer conversions were tracked via Fourier transform infrared spectroscopy (FTIR) as a function of heat treatment conditions (Fig. S7 and fig. S8). As-printed specimens showed nearly complete acrylate conversion in both 405 nm- and 365 nm-cured regions. In contrast, roughly 50% epoxide conversion was achieved in 365 nm-cured regions, while no measurable epoxide conversion was observable in the regions exposed to 405 nm light (Fig. 2E). At higher thermal treatment temperatures and longer hold times, epoxide conversion increased in both visible- and UV-exposed regions, though UV-exposed regions always maintained higher epoxide conversions for any given thermal treatment. Notably, regions exposed to visible light remained soluble, even at epoxide conversion percentages that exceeded those of insoluble UV-exposed samples, indicating dissolution behavior cannot be fully explained in terms of epoxide conversion. We hypothesized that this difference in solubility occurs because purely thermal curing results in lower crosslink densities due to the different mechanisms for light- and heat-driven polymerization. Specifically, reaction conditions during UV light exposure favor chain propagation, while thermally initiated polymerization favors chain transfer and termination (*26*). Because these side reactions can result in the termination of propagating chains or the formation of cyclic oligomers, thermally induced polymerization generates lower crosslink density. Thus, the post-printing thermal treatment of the visible-cured materials results in reduced solvent resistance compared to UV-cured regions, even at the same level of epoxide conversion. While lower crosslink density would be undesirable for the final printed product, it is highly beneficial in the development of dissolvable support structures.

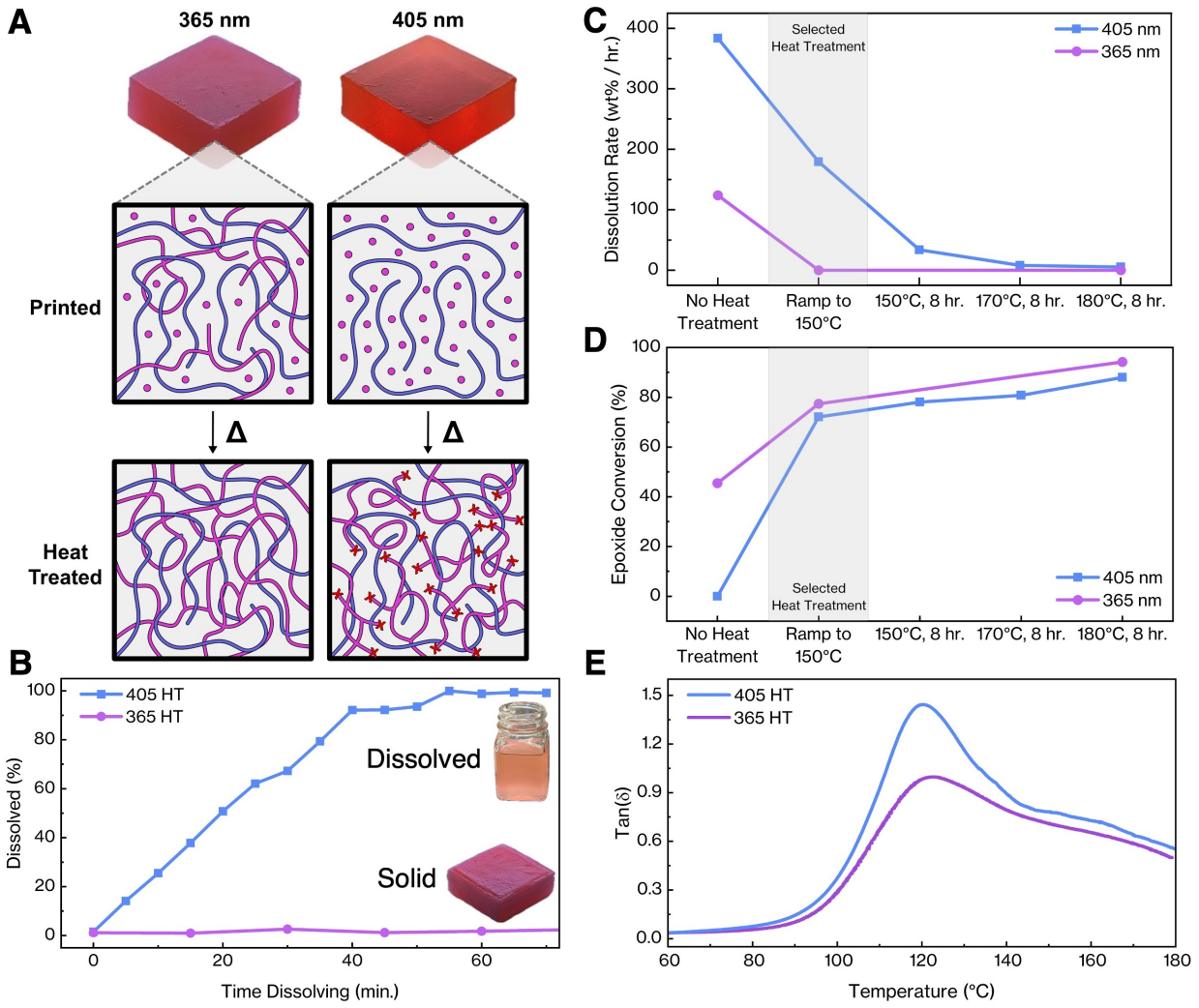

Fig. 2. Heat treatment (HT) after printing ensures a maximum differential in solubility between the two solid phases. (**A**) Samples exposed to visible light form a thermoplastic that contains unreacted epoxide monomers. After thermal treatment, the epoxide monomers react without forming a fully covalently bonded polymer network, allowing the material to be dissolved. On the other hand, samples exposed to UV light form a partially crosslinked polymer network. Thermal treatment of UV samples creates a fully crosslinked network that is highly resistant to dissolution. (**B**) Mass loss of heat-treated parts over time in stirred toluene at ambient conditions. Parts exposed to visible light fully dissolve within an hour, while parts exposed to UV light show no dissolution. (**C**) Dissolution rate of UV and visible prints as a function of post-printing thermal treatment. The gray area shows the processing window used for all prints. (**D**) Epoxide conversion measured using FTIR as a function of thermal treatment. Epoxide conversion scales with increasing time and temperature of heat treatment. (**E**) Dynamic mechanical analysis (DMA) testing. UV parts have a significantly decreased tan(δ) peak height compared to visible-cured parts, which suggests a greater crosslink density for parts exposed to UV light.

DMA experiments on printed, thermally cured samples yielded tan(δ) curves with distinct differences in mechanical response near the glass transition temperature (T_g) of the hybrid material, consistent with the hypothesized differences in polymer network structure (Fig. 2F and Fig. S2). Tan(δ) is equal to the ratio of the loss modulus (dissipated energy) to the storage modulus (elastically stored energy) in a viscoelastic material undergoing oscillatory strain. Physically, low values of tan(δ) correspond to highly elastic materials, while high values of tan(δ) indicate viscous, energy-dissipating behavior. 405 nm-light-exposed samples show a distinct peak in tan(δ) at

approximately 120°C, corresponding with the material's T_g, while 365 nm-exposed samples show this transition a few degrees higher, with significantly reduced peak magnitude. The reduced tan(δ) peak height corresponds to the greater elastic character and lower chain mobility of the UV-exposed material above its T_g, indicating an increased crosslink density relative to the visible-exposed material. The higher mobility of visible-exposed polymer at higher temperatures was also reflected in its greater deflection from plastic flow during DMA (Fig. S9). Additional dissolution experiments supporting the crosslink density hypothesis are detailed in Figure S10.

Recyclability of support material

Although the 405 nm-printed solid primarily consisting of poly(IBOA) is minimally soluble in resin during printing, it can be readily solubilized in pure IBOA at approximately 70°C. This creates a route to recycling the printed support material into new resin that can be repeatedly used in dual-wavelength SSVP (Fig. 3). For this, the printed support material is dissolved in IBOA in amounts up to 15% by mass, followed by filtration to remove particulates, giving a solution containing dissolved poly(IBOA) with small amounts of partially cured EPOX/ECHA (Fig. 3B). Precipitation by adding an excess of isopropanol showed that approximately 60% of the support material's polymeric mass remained dissolved in IBOA, indicating near-full recovery of the acrylate polymer from the original resin which contains ~60 wt% IBOA (see supplemental text). This recycled monomer solution could thus replace IBOA monomer in subsequent resin batches without significantly affecting the resin formulation or printing and dissolution behavior (see supplemental text). This process of support dissolution and reuse was repeatable, with no loss in mechanical properties after repeated recycling (Fig. 3C and Fig. S11).

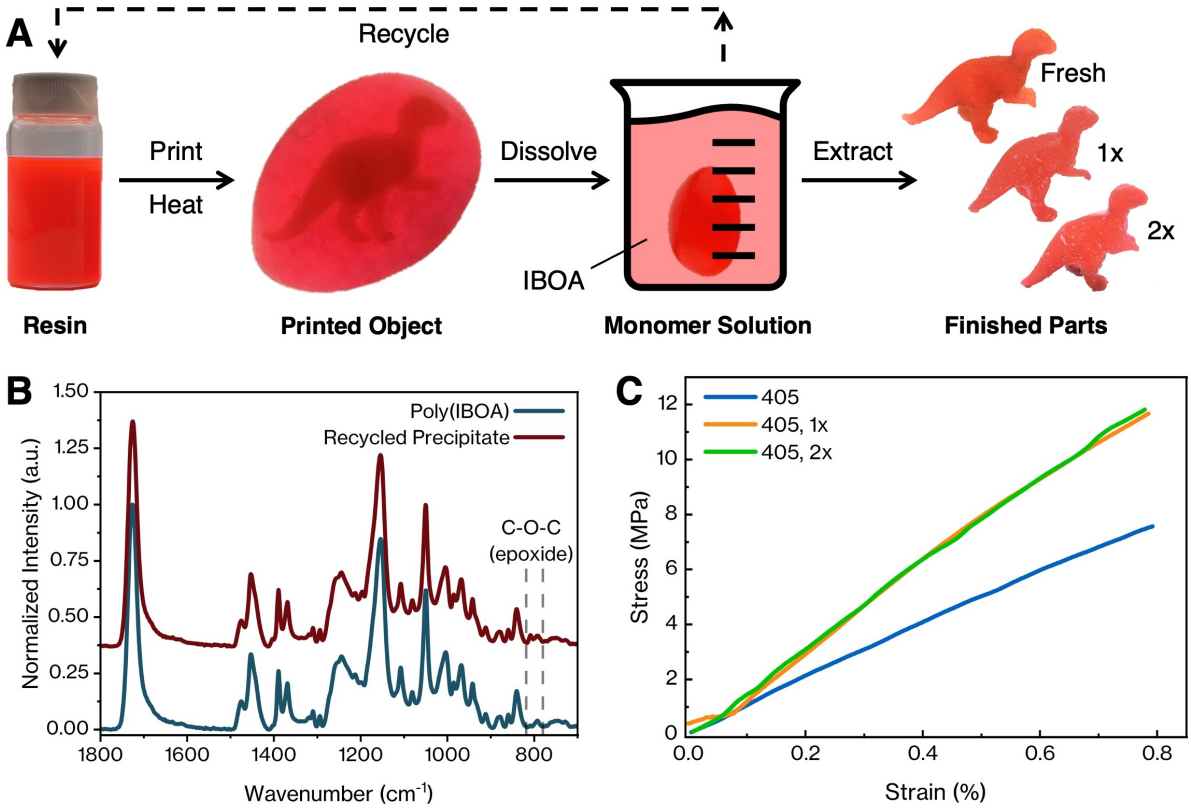

Fig. 3. Demonstration and analysis of support material recycling. (**A**) Support material can be repeatedly dissolved and reused in subsequent resin batches without negatively affecting print quality or mechanical properties, allowing a significant reduction of waste and improved sustainability of the VP process. (**B**) The similarity of FTIR spectra of pure poly(IBOA) and the dissolved polymer for recycling shows that the recycled polymer content is primarily poly(IBOA). (**C**) Representative stress-strain curves of as-printed 405 nm samples over several rounds of recycling. While the first round of recycling leads to an increase in modulus, subsequent recycling rounds lead to mechanical properties that are the same within statistical error.

SSVP of complex geometries

SSVP can realize highly complex geometries and functional assemblies without requiring manual support removal. For example, a functional gear train can be directly produced without any assembly steps (Fig. 4A). Additionally, intricate lattice structures can be fabricated with overhangs that would typically require the removal of extensive internal support structures (Fig. 4B). Parts can also be stacked within the build volume, allowing large numbers of components to be printed simultaneously regardless of their orientation, then released upon support dissolution (Fig. 4C). And, if minimization of the support dissolution time is desirable, the dissolvable material can be printed only at the interface between the crosslinked part and the support structures (Fig. 4D). Here, a denture base is printed by SSVP with dissolvable support interfaces and then mated with a set of artificial teeth printed separately by conventional VP, to form an assembled denture model. Detailed part dimensions are shown in Figure S12.

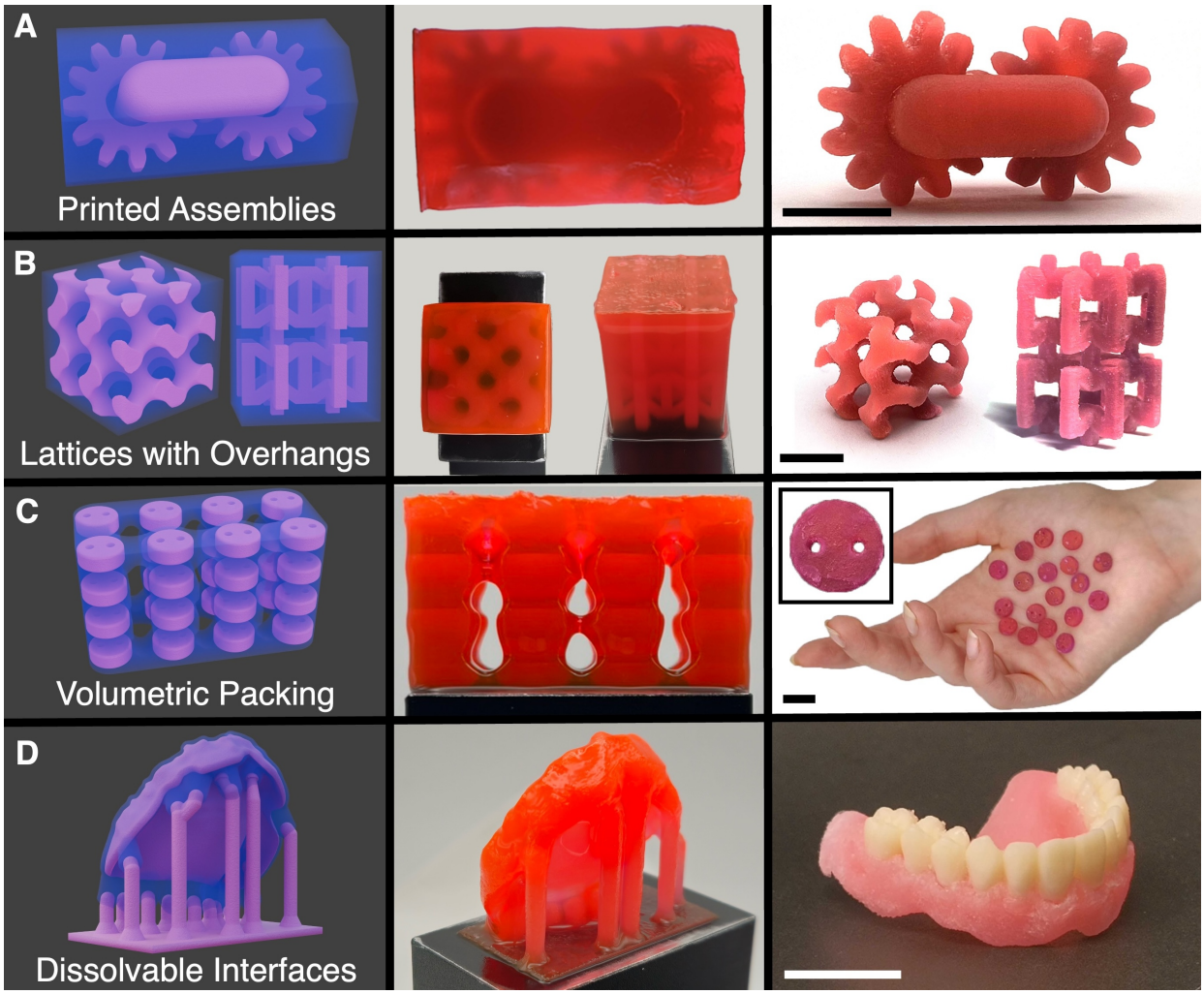

Fig. 4. The results of SSVP printing and post-processing for various complex geometries. From left to right: a rendering of the two-wavelength CAD, the as-printed object, and the object after support dissolution. All scale bars are 1 cm in length. (**A**) A three-part, print-in-place assembly with interlocking, functional gears (Movie S1). (**B**) A gyroid lattice and a reentrant lattice, both with overhanging features that require the use of supports. Support material is dissolved from thin channels in the interior of the lattices. (**C**) Volumetrically packed buttons. The printed support material has channels to reduce resin usage and facilitate solvent access for dissolution. The inset side length is 1 cm. (**D**) A printed denture base and assembled denture model. For this print, only a thin interface between the supports and the object was printed with soluble material. This allows for fast and automatable support removal in a solvent. The teeth inserts were printed with a commercial resin in a separate VP printer, and assembled to the SSVP-printed base.

Finally, SSVP can use wavelength-selective solubility to achieve precise spatial control over dissolution kinetics. For example, spatially and temporally varied UV exposure can produce different degrees of cure and thus different dissolution rates. Demonstrating this concept with a printed 50/50 volume core-shell structure that did not undergo thermal treatment, the outer shell dissolved in ~20 minutes, followed by a slower dissolution of the print's core over ~5 hours (Fig. S13 and S14). Extending this to achieve continuous gradients in dissolution kinetics could be highly applicable to drug delivery and implantable devices.

Alongside the advances presented by SSVP, some limitations must still be overcome to compete with traditional single-vat VP. For example, fine-detailed structures like microfluidics and fabrics are beyond the current resolution limits (Fig. S15 and Fig. S16). However, we

hypothesize that these can be addressed by using printing hardware with higher light intensities. Higher light intensity will also reduce the layer time, increasing overall throughput. Finally, some anisotropic shrinkage occurs during heat treatment, and some anisotropic swelling occurs during dissolution (Fig. S17). We anticipate that efforts to increase the epoxide curing rate and final conversion will alleviate these issues.

Conclusions

By combining wavelength-selective resin design with tailored thermal treatments, SSVP advances photopolymerization 3D printing, enabling the creation of differentially soluble polymer networks within monolithic components. This approach allows for the fabrication of complex internal features without the need for mechanical support removal, eliminating geometric design constraints except for solvent accessibility. Selective solubility could be expanded to additional wavelengths and functionalities, such as locally tuning mechanical, optical, or electronic properties through variable crosslink density. Additionally, SSVP can support fully automated workflows, enabling waste-free mass production via robotic material handling and continuous resin recycling.

References

1. "Standard terminology for additive manufacturing – general principles – terminology" (ASTM ISO/ASTM52900-15, ASTM, 2022).
2. L. Andjela, V. M. Abdurahmanovich, S. N. Vladimirovna, G. I. Mikhailovna, D. D. Yurievich, M. Y. Alekseevna, A review on Vat Photopolymerization 3D-printing processes for dental application. *Dental Materials* **38**(11), e284–e296 (2022). doi:https://doi.org/10.1016/j.dental.2022.09.005
3. Y. L. Yap, W. Y. Yeong, Additive manufacture of fashion and jewellery products: a mini review. *Virtual and Physical Prototyping* **9**(3), 195–201 (2014). doi:10.1080/17452759.2014.938993
4. T. Z. Cui, R. K. Raji, J. L. Han, Y. Chen, Application of 3D printing technology in footwear design and manufacture – a review of developing trends. *Textile & Leather Review* **7**, 1304–1321 (2024). doi:https://doi.org/10.31881/TLR.2024.151
5. M. Nisser, J. Zhu, T. Chen, K. Bulovic, P. Punpongsanon, S. Mueller, "Sequential support: 3D printing dissolvable support material for time-dependent mechanisms" in *Proceedings of the Thirteenth International Conference on Tangible, Embedded, and Embodied Interaction* (Association for Computing Machinery, 2021), 669–676. doi:https://doi.org/10.1145/3294109.3295630
6. B. E. Kelly, I. Bhattacharya, H. Heidari, M. Shusteff, C. M. Spadaccini, H. K. Taylor, Volumetric additive manufacturing via tomographic reconstruction. *Science* **363**(6431), 1075–1079 (2019). doi:10.1126/science.aau7114
7. J. T. Toombs, M. Luitz, C. C. Cook, S. Jenne, C. C. Li, B. E. Rapp, F. Kotz-Helmer, and H. K. Taylor, Volumetric additive manufacturing of silica glass with microscale computed axial lithography. *Science* **376**(6590), 308–312 (2022). doi:10.1126/science.abm6459
8. J. L. Lombardi, D. Popovich, G. J. Artz, Water soluble rapid prototyping support and mold material. U.S. Patent No. US6070107A (2000).
9. A. Bandyopadhyay, B. Heer, Additive manufacturing of multi-material structures. *Materials Science and Engineering R Reports* **129**(17), 1–16 (2018). doi:https://doi.org/10.1016/j.mser.2018.04.001
10. M. Rafiee, R. D. Farahani, D. Therriault, Multi-material 3D and 4D printing: a survey. Advanced *Science* **7**(12), 1902307 (2020). doi:https://doi.org/10.1002/advs.201902307
11. G. Zhu, Y. Hou, J. Xu, and N. Zhao, Reprintable polymers for digital light processing 3D printing. *Advanced Functional Materials* **31**(9), 2007173 (2020). doi:https://doi.org/10.1002/adfm.202007173
12. S. Deng, J. Wu, M. D. Dickey, Q. Zhao, and T. Xie, Rapid open-air digital light 3D printing of thermoplastic polymer. *Advanced Materials* **31**(39), 1903970 (2019). doi:https://doi.org/10.1002/adma.201903970
13. M. D. Alim, K. K. Childress, N. J. Baugh, A. M. Martinez, A. Davenport, B. D. Fairbanks, M. K. McBride, B. T. Worrell, J. W. Stansbury, R. R. McLeod, and C. N. Bowman, A photopolymerizable thermoplastic with tunable mechanical performance. *Materials Horizons* **7**(3), 835–842 (2020). doi:https://doi.org/10.1039/C9MH01336A

14. Z. Xu, R. Hensleigh, N. J. Gerard, H. Cui, M. Oudich, W. Chen, Y. Jing, X. R. Zheng, 2021. Vat photopolymerization of fly-like, complex micro-architectures with dissolvable supports. *Additive Manufacturing* **47**, 102321 (2021). doi: https://doi.org/10.1016/j.addma.2021.102321

15. J. Jin, Y. Chen, Highly removable water support for stereolithography. *Journal of Manufacturing Processes* **28**, 541–549 (2017). doi:https://doi.org/10.1016/j.jmapro.2017.04.023

16. K. L. Sampson, B. Deore, A. Go, M. A. Nayak, A. Orth, M. Gallerneault, P. R. L. Malenfant, C. Paquet, Multimaterial vat polymerization additive manufacturing. *ACS Applied Polymer Materials* **3**(9), 4304–4324 (2021). doi:https://doi.org/10.1021/acsapm.1c00262

17. S. Klimczak, N. Diaco, Digital masking system, pattern imaging apparatus and digital masking method. U.S. Patent No. US11747732B2 (2023).

18. A. Boydston, J. Schwartz, C. Thrasher, T. Becker, M. Ganter, D. Storti, Vat photopolymerization additive manufacturing of multi-material parts. U.S. Patent No. US11518087B2 (2022).

19. U. Shaukat, E. Rossegger, S. Schlögl, A review of multi-material 3D printing of functional materials via vat photopolymerization. *Polymers* **14**(12), 2449 (2022). doi:https://doi.org/10.3390/polym14122449

20. P. Lu, D. Ahn, R. Yunis, L. Delafresnaye, N. Corrigan, C. Boyer, C. Barner-Kowollik, and Z. A. Page, Wavelength-selective light-matter interactions in polymer science. *Matter* **4**(7), 2172–2229 (2021). doi:https://doi.org/10.1016/j.matt.2021.03.021

21. J. J. Schwartz, A. J. Boydston, Multimaterial actinic spatial control 3D and 4D printing. *Nature Communications* **10**(1), 791 (2019). doi:https://doi.org/10.1038/s41467-019-08639-7

22. N. D. Dolinski, Z. A. Page, E. B. Callaway, F. Eisenreich, R. V. Garcia, R. Chavez, D. P. Bothman, S. Hecht, F. W. Zok, C. J. Hawker, Solution mask liquid lithography (SMaLL) for one-step, multimaterial 3D printing. *Advanced Materials* **30**(31), 1800364 (2018). doi:https://doi.org/10.1002/adma.201800364

23. I. Cazin, K. Plevová, W. Alabiso, E. Vidović, S. Schlögl, Dual-wavelength vat photopolymerization 3D printing with hybrid acrylate-epoxy resins: influence of resin composition on microstructure and mechanical properties. *Advanced Engineering Materials* **26**(8), 2301699 (2024). doi:https://doi.org/10.1002/adem.202301699

24. Z. Page, J. W. Kim, M. Allen, H. Cater, A. Uddin, E. Recker, B. Freeman, Hybrid epoxy-acrylate resins for wavelength-selective multimaterial 3D printing. Research Square 4237033 [Preprint] (2024). doi:https://doi.org/10.21203/rs.3.rs-4237033/v1

25. W. Li, M. B. Noodeh, N. Delpouve, J. M. Saiter, L. Tan, M. Negahban, Printing continuously graded interpenetrating polymer networks of acrylate/epoxy by manipulating cationic network formation during stereolithography. *Express Polymer Letters* **10**(12), 1003–1015 (2016). doi:https://doi.org/10.3144/expresspolymlett.2016.93

26. G. Odian, "Ring-Opening Polymerization" in *Principles of Polymerization* (John Wiley & Sons, ed. 4, 2004), pp. 544-618.

27. "Standard test method for assignment of the glass transition temperature by dynamic mechanical analysis" (ASTM E1640-23, ASTM, 2023).

28. “Standard test method for tensile properties of plastics” (ASTM D638-22, ASTM, 2022).

29. R. McCall, 3D Denture, Sketchfab (2018). https://sketchfab.com/3d-models/3d-denture-db38ff23dc534a8c8d27a1107904ef94

30. Q. Hu, G. Lu, K. M. Tse, Tensile mechanical behaviors of re-entrant and kelvin cell lattice structures. *The Journal of The Minerals, Metals & Materials Society* **76**, 387–396 (2024). doi: https://doi.org/10.1007/s11837-023-06193-8

Acknowledgments:

We thank Y. Yam, C.C.L. Wang, and members of the Centre for Perceptual and Interactive Intelligence for helpful discussions. We thank O. Zugay for her expert input on project planning and coordination. We thank A. Namery for her contributions as a hand model. Materials characterization was enabled by the shared instrumentation facilities of MIT.nano and the MIT Materials Research Laboratory, as well as the Institute for Soldier Nanotechnologies, a U.S. Army-sponsored UARC at MIT.

Funding:

InnoCentre AI-based Personalized Product Design and Fabrication project RP5/p5-1 (NSD, KAZ, AJH)

Office of Naval Research Multidisciplinary University Research Initiatives award N00014-23-1-2499 (NSD, CJT, RJM, AJH)

Army Research Office Award W911NF-22-1-0215 (CJT, RJM)

National Science Foundation Graduate Research Fellowship grant 2141064 (NSD, KAZ)

Department of Defense National Defense Science & Engineering Graduate Fellowship Program (CJT)

MIT-Portugal Program (MND)

Author contributions:

Conceptualization: NSD, CJT, AJH

Methodology: NSD, CJT, MMH, MND

Investigation: NSD, MMH, KAZ, MND, SY

Formal Analysis: NSD, MMH, KAZ, MND, SY

Visualization: NSD, CJT, MMH, KAZ, MND

Project Administration: NSD, MMH

Supervision: RJM, AJH

Writing – original draft: NSD, CJT, MMH, KAZ, MND, SY, AJH

Writing – review & editing: NSD, CJT, MMH, RJM, AJH

Competing interests: NSD, CJT, and AJH are listed as inventors on U.S. Patent Application No. 63/724,900, which is related to this research.

Data and materials availability: All data will be made available via DSpace@MIT.

Supplementary Materials

Materials and Methods

Supplementary Text

Figs. S1 to S17

Table S1

References (*1–30*)

Movie S1